viruses

MDPI

Article

Expressing the Pro-Apoptotic Reaper Protein via Insertion into the Structural Open Reading Frame of Sindbis Virus Reduces the Ability to Infect *Aedes aegypti* Mosquitoes

Alexis Carpenter [1], Scott R. Santos [2] and Rollie J. Clem [1,*]

[1] Division of Biology, Kansas State University, Manhattan, KS 66506, USA
[2] Department of Biological Sciences, State University of New York at Buffalo, Buffalo, NY 14260, USA
* Correspondence: rclem@ksu.edu

Abstract: Arboviruses continue to threaten a significant portion of the human population, and a better understanding is needed of the determinants of successful arbovirus infection of arthropod vectors. Avoiding apoptosis has been shown to be one such determinant. Previous work showed that a Sindbis virus (SINV) construct called MRE/rpr that expresses the *Drosophila* pro-apoptotic protein Reaper via a duplicated subgenomic promoter had a reduced ability to orally infect *Aedes aegypti* mosquitoes at 3 days post-blood meal (PBM), but this difference diminished over time as virus variants containing deletions in the inserted *reaper* gene rapidly predominated. In order to further clarify the effect of midgut apoptosis on disseminated infection in *Ae. aegypti*, we constructed MRE/rprORF, a version of SINV containing *reaper* inserted into the structural open reading frame (ORF) as an in-frame fusion. MRE/rprORF successfully expressed Reaper, replicated similarly to MRE/rpr in cell lines, induced apoptosis in cultured cells, and caused increased effector caspase activity in mosquito midgut tissue. Mosquitoes that fed on blood containing MRE/rprORF developed significantly less midgut and disseminated infection when compared to MRE/rpr or a control virus up to at least 7 days PBM, when less than 50% of mosquitoes that ingested MRE/rprORF had detectable disseminated infection, compared with around 80% or more of mosquitoes fed with MRE/rpr or control virus. However, virus titer in the minority of mosquitoes that became infected with MRE/rprORF was not significantly different from control virus. Deep sequencing of virus populations from ten mosquitoes infected with MRE/rprORF indicated that the *reaper* insert was stable, with only a small number of point mutations and no deletions being observed at frequencies greater than 1%. Our results indicate that expression of Reaper by this method significantly reduces infection prevalence, but if infection is established then Reaper expression has limited ability to continue to suppress replication.

Keywords: apoptosis; Sindbis virus; arbovirus; alphavirus; antiviral immunity; mosquito; vector competence

Citation: Carpenter, A.; Santos, S.R.; Clem, R.J. Expressing the Pro-Apoptotic Reaper Protein via Insertion into the Structural Open Reading Frame of Sindbis Virus Reduces the Ability to Infect *Aedes aegypti* Mosquitoes. *Viruses* **2022**, *14*, 2035. https://doi.org/10.3390/v14092035

Academic Editor: Richard J. Kuhn

Received: 13 May 2022
Accepted: 9 September 2022
Published: 13 September 2022

1. Introduction

Recent decades have seen the emergence and reemergence of a number of significant arboviral diseases such as dengue, Zika, West Nile, yellow fever, and chikungunya [1–3]. Arboviruses, which are transmitted through the bite of an infected arthropod vector such as a tick or mosquito, are expected to become more significant in the future and it is predicted that climate change will increase incidence of disease by impacting vector geographical range, feeding behavior, and survival [4–6]. New ways of protection from these diseases are needed as vaccines are not available for many of these diseases and there is increasing insecticide resistance in some vectors [7–9].

An alternative to traditional means of controlling arboviral diseases is to prevent productive infection of the vector. Tissue barriers in the vector such as the midgut present an obstacle for viruses to overcome and inhibiting escape from midgut tissue would prevent

disseminated infection and thus the spread of these viruses [10]. Several pathways and processes may be considered which when altered could prevent disseminated infection, and improved knowledge of these pathways could lead to new strategies of vector infection control. One cellular process which shows potential promise in preventing disseminated infection is apoptosis, a specific type of programmed cell death that has been shown to be an important antiviral pathway in many organisms including insects [11,12]. The insect apoptosis pathway has been best studied in *Drosophila melanogaster*, but a similar pathway has been demonstrated in the disease vector *Aedes aegypti* [13–16]. During apoptosis, activated initiator caspases cleave and activate effector caspases, which are responsible for cleaving target proteins in the cell, leading to death. Activation of initiator caspases is prevented by inhibitor of apoptosis (IAP) proteins, the action of which can be overcome by IAP antagonists such as *Drosophila* Reaper, which can bind directly to IAP proteins via the IAP binding motif (IBM) found at its amino terminus [17]. The result is a carefully controlled mechanism which prevents unnecessary cell death but promotes cell death in response to activating stimuli such as viral infection.

The role of apoptosis in protecting insects against viral infections brings up the question of what role it plays in vector competence for arboviruses. Several studies have implicated apoptosis as a significant factor in preventing viral escape from the midgut. For example, enhanced midgut apoptosis has been associated with a *Culex pipiens pipiens* strain of mosquitoes that were refractory to West Nile virus infection [18]. Additionally, previous work by our group showed that a SINV construct that expressed Reaper from a duplicated subgenomic promoter was initially less able to infect and disseminate from the *Ae. aegypti* midgut, although viruses with deletions in the *reaper* insert rapidly predominated [19]. Consistent with these results, one study showed that some pro-apoptotic genes were more highly expressed in a refractory strain compared to a susceptible strain of *Ae. aegypti* [20], while another study found increased rapid induction of apoptosis in mosquitoes that were less susceptible to dengue virus serotype 2 (DENV-2) compared to a more susceptible strain [21]. However, it has also been suggested that excessive apoptosis may weaken the barrier that the midgut provides and thus allow viruses to pass through more easily. One study found that knocking down AeIAP1 expression in *Ae. aegypti* and then feeding them with SINV led to increased midgut infection and virus dissemination [22]. Due to a high rate of mosquito mortality in these AeIAP1 knockdown mosquitoes, it was hypothesized that the level of apoptosis was drastically increased, greatly reducing the structural integrity of the midgut. It is possible that some level of apoptosis is critical to preventing virus passage through tissues but if apoptosis levels are too high, viral spread is promoted through gaps in the structure.

A previous series of studies by our group aimed to determine how inserting the *Drosophila* pro-apoptotic gene *reaper* into SINV and then infecting *Ae. aegypti* would affect rates of disseminated infection [19,23]. The construct used in these earlier studies, called MRE/rpr, expressed Reaper via a duplicated subgenomic promoter located between the nonstructural and structural genes. MRE/rpr strongly induced apoptosis and had decreased virus yield compared to control viruses in cultured mosquito cells [23]. When mosquitoes were fed MRE/rpr, apoptosis was observed in midgut cells and it was found that there was less disseminated infection compared to control virus at early time points, but by 7 days post-blood meal (PBM), there was no significant difference between MRE/rpr and control. The reason for this was found to be that a significant proportion of the MRE/rpr population by 7 days PBM had deletions in the *reaper* insert, rendering it nonfunctional [19]. This result indicated strong negative selection against Reaper expression and supported a role for apoptosis as an antiviral response. However, the lack of stability of Reaper expression from MRE/rpr complicates the interpretation of these results.

To potentially deliver more stable expression of Reaper protein, we decided to insert the *reaper* gene into the structural ORF of SINV, a method which has been previously shown to allow more stable insertions into the SINV genome [24,25]. By inserting the sequence into the structural ORF as a continuous open reading frame between the capsid

gene and PE2, as opposed to the duplicated subgenomic promoter region, we hoped to increase selective pressure for retaining the insert because deletions in *reaper* would be more likely to negatively impact the expression of critical viral structural proteins. To allow proper synthesis of the viral structural proteins, we utilized the autoproteolytic function of the SINV capsid protein and the ribosomal skipping function of foot and mouth disease virus (FMDV) 2A [26] to cotranslationally release the Reaper protein. Additionally, we employed a ubiquitin fusion strategy which has been used successfully to generate proteins with precise N-terminal sequences [27,28]. This ensured that we would not impact the N-terminus of Reaper, which has been shown to be critical for binding IAPs [17].

Using this SINV construct, called MRE/rprORF, we then re-examined the effect of Reaper expression on establishment of midgut infection and dissemination from the midgut. Our results provide deeper insights into the effects of apoptosis on SINV infection in *Ae. aegypti*.

2. Materials and Methods

2.1. Cells

BHK-21 cells were maintained at 37 °C with 5% CO_2 in Dulbecco modified Eagle medium (DMEM, Gibco, Waltham, MA, USA) plus 10% fetal bovine serum (FBS, Atlanta Biologicals, Minneapolis, MN, USA). C6/36 cells were maintained at 27 °C in Liebovitz's medium (Gibco) plus 10% FBS.

2.2. Insect Rearing

Orlando strain *Ae. aegypti* mosquitoes (obtained in 2008 from James Becnel, USDA ARS, Gainesville, FL, USA) were reared in a 27 °C incubator with 80% humidity and a 12-h light-dark cycle. To obtain eggs used in experiments, females were allowed to feed on defibrinated sheep's blood (Colorado Serum Company, Denver, CO, USA) using a Hemotek feeding system (Hemotek Ltd., Blackburn, UK). Adult mosquitoes were maintained on raisins and water.

2.3. Plasmid Design and Construction

A previously described plasmid containing a fragment of 5′dsMRE16ic extending from the NotI site to the AvrII site as well as microRNA target sites and a 2A self-cleaving peptide sequence ligated into a pGEM-T backbone was used as the starting plasmid [25]. This plasmid was digested with BstEII and AfIII and the intervening sequence containing the miRNA target sites was replaced with the following sequence (synthesized by Genewiz, South Plainfield NJ) containing ubiquitin (human K48R), the *Drosophila reaper* sequence (lacking the initiator methionine), and an HA tag: (TGGAATAGCAAGGGAAAGACCATCAAGAC-GACGCCCGAAGGGACAGAGGAATGGTCAGCAGCACTCGAGATGCAGATCTTCGTC AAGACGTTAACCGGTAAAACCATAACTCTAGAAGTTGAACCATCCGATACCATCGA AAACGTTAAGGCTAAAATTCAAGACAAGGAAGGCATTCCACCTGATCAACAAAGA TTGATCTTTGCCGGTAGGCAGCTTGAGGACGGTAGAACGCTGTCTGATTACAACATT CAGAAGGAGTCCACCCTGCACCTGGTCCTCCGTCTCAGAGGTGGTGCAGTGGCATT CTACATACCCGATCAGGCGACTCTGTTGCGGGAGGCGGAGCAGAAGGAGCAGCAG ATCCTTCGCTTGCGGGAGTCACAGTGGAGATTCCTGGCCACCGTCGTCCTGGAAAC CCTGCGCCAGTACACTTCATGTCATCCGAAGACCGGAAGAAAGTCCGGCAAATATC GCAAGCCATCGCAATACCCATACGATGTTCCAGATTACGCTGGATCCCAGCTGTTGA ATTTTGACCTT). A control plasmid was generated in the same way, but the intervening sequence was replaced with a synthesized sequence not containing *Drosophila reaper* but still containing ubiquitin and an HA tag: (TGGAATAGCAAGGGAAAGACCATCAAGAC-GACGCCCGAAGGGACAGAGGAATGGTCAGCAGCACTCGAGATGCAGATCTTCG TCAAGACGTTAACCGGTAAAACCATAACTCTAGAAGTTGAACCATCCGATACCATC GAAAACGTTAAGGCTAAAATTCAAGACAAGGAAGGCATTCCACCTGATCAACAAA GATTGATCTTTGCCGGTAGGCAGCTTGAGGACGGTAGAACGCTGTCTGATTACAAC ATTCAGAAGGAGTCCACCCTGCACCTGGTCCTCCGTCTCAGAGGTGGTTATCCATAC

GATGTTCCAGATTACGCTGGATCCCAGCTGTTGAATTTTGACCTT). Both plasmids were then digested with NotI and AvrII and the purified fragments were ligated into p5′dsMRE16ic which had been digested with the same restriction enzymes. Proper insertion was verified by Sanger sequencing. The generation of MRE/rpr has previously been described [23].

2.4. Virus Production

Infectious clone plasmids were linearized using AscI (New England Biolabs, Ipswich, MA, USA) and then in vitro transcribed using the MEGAscript SP6 transcription kit (Thermo Fisher Scientific, Waltham, MA, USA) with added cap analog (New England Biolabs). Following transcription, RNA was transfected into BHK-21 cells using Lipofectamine 3000 (Thermo Fisher Scientific). After two days, the media was removed and used to infect a T75 flask of C6/36 cells. After 5 days, the resulting P2 virus stock was frozen in aliquots and titer was determined using $TCID_{50}$ assay.

2.5. $TCID_{50}$ Assay

BHK-21 cells were plated at a density of 1×10^4 cells per well in a 96-well tissue culture plate in 100 µL of DMEM plus 10% FBS and supplemented with 15 µg per ml of penicillin/streptomycin (Invitrogen, Waltham MA). Mosquito and cell samples were removed from −80 °C and thawed on ice. Samples were then spun to remove debris and DMEM was used to make serial dilutions of each sample. Each dilution was transferred to five wells containing BHK-21 cells. After 5 days, each well was scored for cytopathic effects. The number of wells of each dilution scored as positive was used to determine $TCID_{50\,mL}{}^{-1}$ and this was converted to PFU mL^{-1} by multiplying by 0.69 [29].

2.6. Replication Curves

For replication curves in C6/36 cells, the cells were plated at a density of 1×10^6 cells per well in a 6-well plate in 2 mL of Leibovitz's medium containing 10% FBS. For replication curves in BHK-21 cells, the cells were plated at a density of 5×10^5 cells per well in a 6-well plate in 2 mL DMEM containing 10% FBS. Cells were allowed to recover for 2 h and then were infected with MRE/rprORF, MRE/rpr, or MRE/control at a multiplicity of infection (MOI) of 0.1. The cells were placed on a rocker and the virus was allowed to adsorb for 1 h. The media was then removed, and the cells were rinsed before replacing the media. For the cumulative replication curves, 100 µL of media was sampled for analysis at 1, 2, 3, and 4 dpi. For the non-cumulative replication curves, 100 µL of media was sampled at each time point for analysis and then the remaining media was removed, the cells were rinsed twice, and then 2 mL of media were added. All samples were frozen and stored at −80 °C until analysis by $TCID_{50}$ assay.

2.7. DNA Fragmentation Assay

C6/36 cells were plated at a density of 2×10^6 cells per well in a 6-well plate in 2 mL Leibovitz's medium containing 10% FBS. Cells were allowed to recover for 2 h and then were infected with MRE/rprORF, MRE/control, or 5′dsMRE16ic at an MOI of 1. After 48 h, cells were removed from the 6-well plates and pelleted at 500× *g*. They were washed twice with phosphate buffered saline (140 mM NaCl, 2.7 mM KCl, 10 mM Na2HPO4, 1.8 mM KH2PO4) and then resuspended in 200 µL lysis buffer (0.1 M SDS, 0.1 M Tris pH 8.0, 0.05 M EDTA pH 8.0, 200 mg ml^{-1} Proteinase K) and incubated at room temperature for 1 h. The samples were then extracted twice with phenol/chloroform and then ethanol precipitated. The pelleted DNA was resuspended in 100 µL Tris-EDTA buffer (10 mM Tris-Cl, 1 mM EDTA) containing 100 µg mL^{-1} RNase A (Thermo Fisher Scientific) and incubated at room temperature for 5 min. Twenty µL of each sample was loaded into a 1.2% agarose gel containing 0.5 µg mL^{-1} ethidium bromide. The gel was visualized using an AlphaImager gel imaging system (Alpha Innotech, San Leandro, CA, USA). Sizes of the bands were compared to a Versaladder DNA ladder (Gold Bio, Olivette, MO, USA).

2.8. Mosquito Infection for $TCID_{50}$ and Caspase Assay

Prior to blood feeding, mosquitoes were placed in cups containing 20–30 females and 10% males and were only provided water for 24 h. MRE/rprORF, MRE/rpr, and MRE/control stocks were diluted to 1.45×10^7 PFU mL^{-1} with Liebovitz's medium. The diluted virus stocks were then mixed 1:1 with defibrinated sheep blood and the mosquitoes were then allowed to feed on one of the virus blood mixtures using a Hemotek feeding system for 90 min. Fully engorged females were separated from unfed and partially fed females and males and were given water and raisins to feed *ad libitum*. At 3, 5, and 7 days PBM, the mosquitoes were cold anesthetized, and the midguts were dissected from the rest of the mosquito (the carcass). The midguts and carcasses used for $TCID_{50}$ assays were placed in 1.5 mL tubes containing 200 µL DMEM media containing 10% FBS and homogenized using disposable pestles. The samples were then frozen at −80 °C. The midguts used for caspase assays were collected in 30 µL of caspase reaction buffer (20 mM Hepes-KOH, pH 7.5, 50 mM KCl, 1.5 mM MgCl2, 1 mM EDTA, 1 mM EGTA, 1 mM DTT), homogenized with disposable pestles, and stored at −80 °C.

2.9. Immunoblotting

C6/36 cells were plated at a density of 2×10^6 cells per well in a 6-well plate containing 2 mL Leibovitz's media plus 10% FBS. They were then infected with MRE/rprORF, MRE/control, or 5′dsMRE16ic at an MOI of 10. After 24 or 48 h, the cells were rinsed three times with cold PBS. The plate was placed on ice and 100 µL of cold Laemmli sample buffer (Bio-Rad, Hercules CA) was added to each well. The wells were scraped, and the lysate was collected in a 1.5 mL tube. The samples were then heated to 100 °C for 5 min, centrifuged at 4 °C, and the supernatant was transferred to a new tube. SDS-PAGE was performed using 30 µL of sample with 4–20% Bis-Tris gels (Genscript, Piscataway, NJ, USA) in Tris-MOPS-SDS running buffer (Genscript), and proteins were transferred to PVDF membrane. After blocking for 1 h in 5% dried skim milk in TBST, a 1:1000 dilution of the anti-HA (Biolegend, San Diego, CA, USA) or anti-β-actin (Santa Cruz Biotechnology, Dallas, TX, USA) primary antibody was incubated with the membrane overnight at 4 °C with constant agitation. After incubation, the membrane was washed three times with TBST. A 1:15,000 dilution of goat anti-mouse IgG-horseradish peroxidase secondary antibody (Thermo Fisher Scientific) was added and was incubated for 1 h at room temperature with agitation. Bands were detected using SuperSignal West Pico PLUS Chemiluminescent Substrate (Thermo Fisher Scientific) and visualized using a LI-COR Western Blot Imager.

2.10. Caspase Assay

In the cell experiments, C6/36 cells were plated at a density of 2×10^6 cells per well in a 6-well plate in 2 mL Leibovitz's media plus 10% FBS. The cells were infected with MRE/rprORF, MRE/rpr, or MRE/control at an MOI of 1. At 24 and 48 hpi, the cells were rinsed with PBS and then collected in 400 µL of caspase reaction buffer. Mosquito midgut samples were collected in pools of 8 in caspase reaction buffer and the tissues were disrupted by sonication. The tubes were centrifuged, and the supernatant was moved to a new tube. All samples were frozen at −80 °C until testing. Bradford protein assay (Bio-Rad) was used to determine protein concentration, and cell and mosquito samples were diluted to 100 µg ml^{-1}. A total of 50 µL of each sample were added to white 96-well plates (Costar; Sigma Aldrich, St. Louis, MO, USA) and incubated at 37 °C for 15 min. Then, 10 µL of Ac-DEVD-AFC (ApexBio, Houston, TX, USA) was added to each well at a final concentration of 20 µM. Cleavage of this fluorogenic substrate was monitored at an excitation wavelength of 405 nm and an emission wavelength of 535 nm using a Victor3 1420 Multilabel Counter (Perkin-Elmer, Waltham, MA, USA). Readings were taken at 15 min intervals for a period of 1 h.

2.11. Deep Sequencing of Virus Populations

Total RNA was isolated using TRIzol (Invitrogen) from the carcasses of 10 mosquitoes that became infected with MRE/rprORF and were harvested at 5 or 7 days PBM, as well as from the same MRE/rprORF stock virus that was used in mosquito infections. Samples C6, C9, C20, C24, C36, and C37 were from 5 days PBM, while C11, C17, C18, and C19 were from 7 days PBM. RNA was converted to cDNA using the Improm-II reverse transcription system (Promega) and oligo dT primer. The resulting cDNA was subjected to PCR using Q5 high fidelity polymerase (New England Biolabs) with primers that amplified a ~450 bp region of the MRE/rprORF genome containing the *reaper* sequence (forward primer: 5′- TCGTCGGCAGCGTCAGATGTGTATAAGAGACAGTACAACATTCAGAAGGAGTCC AC-3′; reverse primer: 5′- GTCTCGTGGGCTCGGAGATGTGTATAAGAGACAGGTCATA TTTCCCAGGATGCAC-3′). The primers also included Illumina overhang adaptor sequences. PCR products were purified and used for index PCR. Following validation and quantification, amplicons were purified, pooled, and sequenced via 2 × 300 bp Illumina MiSeq at the K-State Integrated Genomics Facility.

Paired end reads were remapped to the 5′dsMRE16ic reference genome using BWA 0.7.17-r1198-dirty under the BWA-MEM algorithm [30]. The resulting SAM file was converted to binary format, sorted, and indexed using SAMtools v1.10 [31]. Variant calling was done using bam-readcount 0.8.0-unstable-7-625eea2 [32] with filtering and removal of false-positive calls having minimum base and mapping qualities of less than 30 and 20, respectively. Output from bam-readcount was converted to tab-delimited files which are presented as Data Set S1. Sequence data have been deposited in the Sequence Read Archive under BioProject ID PRJNA875102.

3. Results

3.1. MRE/rprORF Virus Construction and Reaper Expression

To generate a SINV construct with potentially enhanced stability of the pro-apoptotic gene *reaper*, we inserted this gene into the structural ORF of the 5′dsMRE16ic infectious clone [33] (Figure 1A). The resulting construct, which we named MRE/rprORF, has *reaper* and flanking sequences inserted immediately after the capsid gene (Figure 1B). To ensure proper processing of both Reaper and the SINV capsid and E2 proteins, the first sequence inserted after the capsid gene was the first three codons of PE3, which are required for an intact capsid autoproteolytic cleavage site. However, this created a problem because these three amino acids would be fused to the Reaper protein, and the N-terminus of Reaper has been shown to be critical for its function in binding IAPs [17]. Following normal translation of cellular Reaper, methionyl peptidases remove the N-terminal methionine, revealing an alanine that is required for binding to IAPs [34]. To avoid this problem, we used a ubiquitin-Reaper fusion strategy. After the three PE3 codons, we inserted a ubiquitin gene immediately followed by the *reaper* gene (lacking the N-terminal methionine) with a hemagglutinin (HA) epitope tag at its C-terminus to facilitate detection of Reaper expression. Cellular proteases cleave ubiquitin fusion proteins immediately following the ubiquitin sequence [27]. Thus, the insertion of ubiquitin would result in expression of Reaper with amino-terminal alanine. Following HA-tagged *reaper*, we inserted the FMDV 2A sequence which causes ribosomal skipping [26] and thus should free the Reaper protein from the rest of the polypeptide chain. The result was a predicted Reaper-HA fusion protein expressed from the structural ORF that allows for intact viral structural protein processing. As a control virus, we constructed MRE/control, which contained the same elements described above but lacked the *reaper* sequence (Figure 1B). The other constructs used in this study were MRE/rpr (Figure 1C), which has been previously described and expresses Reaper via a duplicated subgenomic promoter, and the parental clone 5′dsMRE16ic (Figure 1A), which also has been previously described and did not contain any of the inserted sequences other than the duplicated subgenomic promoter present in all of the constructs [19,23,33].

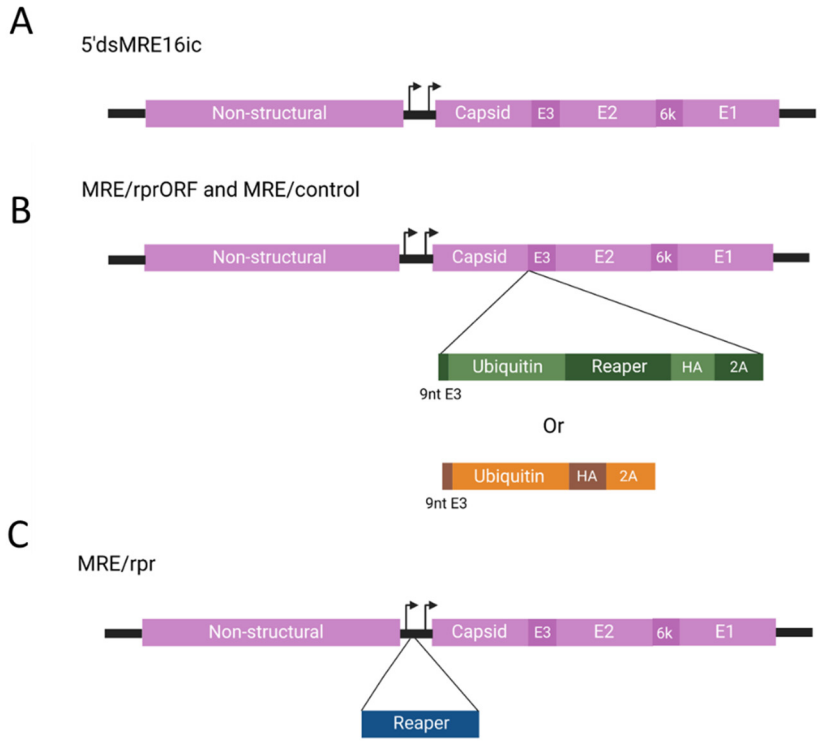

Figure 1. Diagrams of virus constructs used in this study (not drawn to scale). (**A**) 5′dsMRE16ic was used as the starting backbone for the other viruses and does not contain any inserted sequences in the duplicated subgenomic promotor region or the structural ORF. Arrows indicate subgenomic promoter transcription start sites. (**B**) MRE/rprORF and MRE/control contain sequences inserted after the final codon of the capsid sequence in the structural ORF. In both constructs, the first nine nucleotides of PE3 are duplicated following the capsid to allow autoproteolytic activity of the capsid. Immediately following the PE3 insertion, MRE/rprORF contains a ubiquitin-reaper fusion with an HA tag. MRE/control contains ubiquitin and HA but does not contain *reaper*. The inserted sequence of both constructs ends with FDMV 2A which will release peptides as they are translated. (**C**) MRE/rpr contains the *reaper* gene inserted in the duplicated subgenomic promoter region. The figure was created with Biorender.com.

After these viruses were constructed, we first confirmed expression of the Reaper protein from MRE/rprORF by immunoblotting (Figure 2). C6/36 cells were infected with MRE/rprORF, 5′dsMRE16ic (labeled MRE16 in the figure), or MRE/control, or they were mock infected, and at 24 or 48 h post-infection (hpi), protein was isolated and HA-tagged proteins were detected by immunoblotting. At 24 hpi, we detected an HA-reactive protein in MRE/rprORF-infected cells of about 18 kDa. This likely represents uncleaved ubiquitin-Reaper fusion protein, which is predicted to be around this size. At 48 hpi, lysates from cells infected with MRE/rprORF still contained the 18 kDa protein but in addition had another protein of around 9 kDa, which likely corresponds to the HA-tagged Reaper protein after cleavage from ubiquitin. No proteins of similar size were detected in any of the other treatments. We also observed an HA-immunoreactive band of about 57 kDa at both time points in MRE/control-infected cells, as well as some faster migrating bands at 48 hpi (Figure S1). Because in this control construct the HA tag is located immediately downstream of ubiquitin, we speculate that these bands may correspond to ubiquitin that was still fused to the HA tag and had been conjugated to unknown protein(s) by ubiquitin ligases. We did not observe any replication deficit in these constructs (see Figure 4), suggesting that the expression of ubiquitin did not significantly affect virus replication. A protein of about 72 kDa that was seen in all treatments (Figure S1) was assumed to be of cellular origin and detected as the result of antibody cross-reactivity.

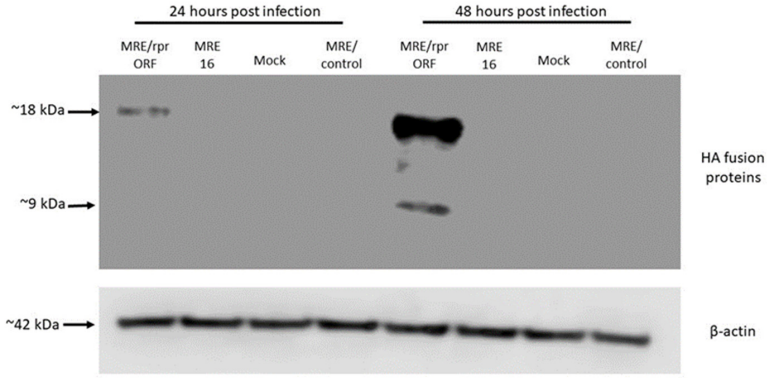

Figure 2. MRE/rprORF expresses the Reaper protein in infected cells. C6/36 cells were infected with MRE/rprORF, 5′dsMRE16ic (labeled MRE16), or MRE/control, or were mock infected and protein was extracted at 24 and 48 hpi. Immunoblotting was done using antibodies against HA (**upper panel**) or β-actin as a loading control (**lower panel**).

3.2. MRE/rprORF Causes Increased Apoptosis in C6/36 Cells

To confirm that the Reaper protein expressed from MRE/rprORF was functional, we infected cells with this virus and then tested for markers of apoptosis, as was previously done for MRE/rpr [23]. We first demonstrated stimulation of apoptosis by MRE/rprORF infection using a chromatin fragmentation assay (Figure 3A). Endonucleolytic chromatin fragmentation (or nucleosomal laddering), which is characterized by the appearance of a ladder-like pattern on gel electrophoresis, has long been known to be a hallmark of apoptotic cells [35–37]. A nucleosomal ladder in multiples of approximately 140 bp was evident at 48 hpi in C6/36 cells that were infected with MRE/rprORF, while DNA from cells that were infected with MRE/control or 5′dsMRE16ic (abbreviated as MRE16) did not display this pattern. We also demonstrated increased apoptosis in these cells using a caspase assay which measures effector caspase activity by detecting increased cleavage of a fluorogenic substrate, Ac-DEVD-AFC (Figure 3B). We did not find differences in caspase activity (slope of the lines) between cells infected with MRE/rprORF, MRE/control, or MRE/rpr when they were collected at 24 hpi. However, at 48 hpi, cells infected with MRE/rprORF or MRE/rpr were found to have increased effector caspase activity when compared to MRE/control. This increase between 24 and 48 hpi correlates with the levels of Reaper expression in MRE/rprORF-infected cells as determined by immunoblotting (Figure 2).

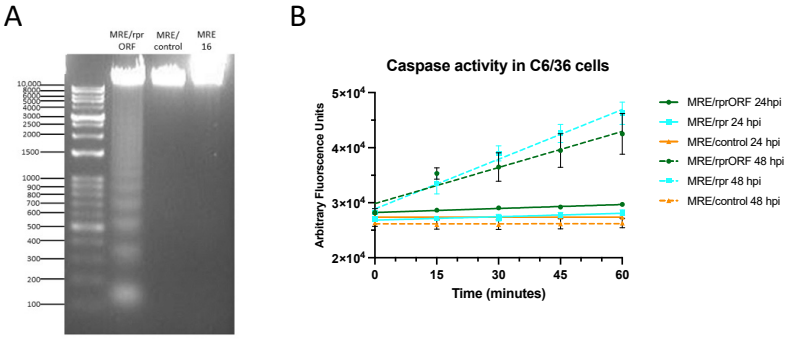

Figure 3. MRE/rprORF causes apoptosis in C6/36 cells. (**A**) C6/36 cells were infected with MRE/rprORF, MRE/control, or 5′dsMRE16ic (labeled MRE16). After 48 h, the cells were collected, DNA was extracted, and run on an agarose gel containing ethidium bromide. (**B**) Cells infected with MRE/rprORF, MRE/rpr, or MRE/control were collected and lysed at 24 and 48 hpi. Caspase activity from these cell lysates was measured by examining their ability to cleave the fluorogenic substrate Ac-DEVD-AFC. Fluorescence measurements were taken every 15 min for 1 h. Three biological replicates were performed. The data were plotted using simple linear regression. Error bars indicate SEM.

3.3. MRE/rprORF and MRE/rpr Show Replication Differences Compared to Control SINV in BHK-21 and C6/36 Cells

To determine how Reaper expression would affect SINV replication and whether the insertion site of *reaper* in the viral genome would influence this effect, we infected BHK-21 and C6/36 cells and sampled the cell culture media by median tissue culture infectious dose ($TCID_{50}$) assay at several time points to construct replication curves (Figure 4). In BHK-21 cells, we found that MRE/rprORF and MRE/rpr had reduced titers compared to MRE/control at most time points, with the largest difference being at 4 days post-infection (dpi) (Figure 4A). There was no significant difference between the MRE/rprORF and MRE/rpr replication curves. In C6/36 cells, we constructed a cumulative replication curve as well as a non-cumulative replication curve in which the cells were rinsed after sampling at each time point (Figure 4B). In the cumulative replication curve, both MRE/rprORF and MRE/rpr had lower titers than MRE/control at most time points and the differences were found to increase at later time points from about 10-fold at 2 dpi to around 100-fold at days 3 and 4. Differences between MRE/rprORF and MRE/rpr were not found to be significant. In the non-cumulative replication curve, MRE/rprORF and MRE/rpr titers were similar to MRE/control at early time points but the Reaper-expressing viruses diverged from MRE/control at the later time points of 4 and 5 dpi. Titers of MRE/control remained near 10^8 PFU mL^{-1} after 3 dpi, while MRE/rprORF and MRE/rpr titers reached between 10^7 and 10^8 PFU mL^{-1} at 3 dpi and then declined at 4 and 5 dpi. This decrease was expected since the Reaper-expressing viruses were causing apoptosis by these later time points. The replication curve of MRE/rprORF was found to be significantly different from MRE/rpr, with MRE/rprORF showing a more drastic decline after peaking at 3 dpi.

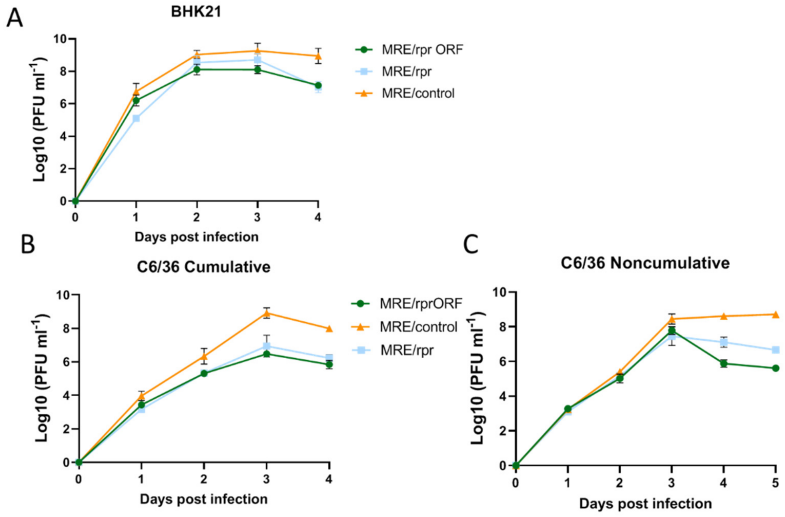

Figure 4. Virus replication curves in BHK-21 and C6/36 cells. (**A**,**B**) BHK-21 or C6/36 cells were infected with MRE/rprORF, MRE/rpr, or MRE/control at MOI 0.1 and a sample of supernatant was removed and titered by $TCID_{50}$ assay at each of the indicated time points. (**A**) In BHK-21 cells, MRE/rprORF ($p = 0.003$) and MRE/rpr ($p = 0.0002$) were significantly different compared to MRE/control. MRE/rpr and MRE/rprORF were not significantly different ($p = 0.9879$). (**B**) In C6/36 cells, MRE/rprORF ($p < 0.0001$) and MRE/rpr ($p < 0.0001$) were significantly different compared to MRE/control. MRE/rprORF and MRE/rpr were not significantly different ($p = 0.7702$). (**C**) Non-cumulative replication curve. C6/36 cells were infected with MRE/rprORF, MRE/rpr, or MRE/control at MOI 0.1. At each indicated time point, a sample of supernatant was removed for $TCID_{50}$ assay. The remaining cell culture medium was then removed from each well, the cells were rinsed, and the media was replaced. MRE/rprORF ($p < 0.0001$) and MRE/rpr ($p < 0.0001$) were significantly different compared to MRE/control. MRE/rprORF and MRE/rpr were also significantly different ($p = 0.0291$). In (**A**–**C**), three independent biological replicates were performed. Titers were log transformed and compared with two-way ANOVA and Tukey's multiple comparison test. Error bars represent SEM.

3.4. Mosquitoes That Ingest Blood Containing MRE/rprORF Show Increased Caspase Activity in Midgut

We next wanted to see if we would find evidence of apoptosis in mosquitoes after they fed on blood containing the MRE/rprORF virus. In this experiment, we allowed mosquitoes to feed on blood with MRE/rprORF, MRE/rpr, or MRE/control. After three days, the mosquitoes were dissected and pools of eight midguts from each treatment were tested for effector caspase activity. We found that there were significant differences in effector caspase activity between the three treatments by two-way ANOVA (Figure 5). Pooled midguts from the mosquitoes that fed on blood containing MRE/rprORF had the highest effector caspase activity as indicated by the increase in fluorescence over time. Together with our previous demonstration that Reaper expression by MRE/rpr causes increased apoptotic cells in midgut by TUNEL staining [19], this increased effector caspase activity suggests that infection with MRE/rprORF also induced apoptosis in midgut. Caspase activity in MRE/rpr-exposed midguts was only marginally higher than in midguts exposed to MRE/control at this time point, suggesting that MRE/rprORF induced apoptosis at a higher level than MRE/rpr.

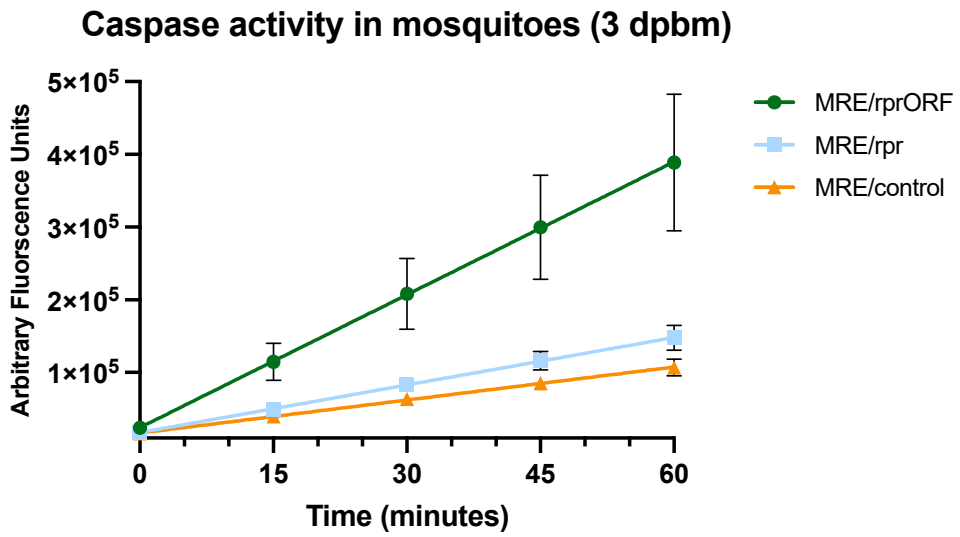

Figure 5. MRE/rprORF causes increased effector caspase activity in *Ae. aegypti* midgut. Mosquitoes were fed blood containing MRE/rprORF, MRE/rpr, or MRE/control and midguts were dissected after 3 days. Midguts were pooled in groups of eight with three pools/treatment. Each pool thus represents an independent biological replicate. Cells were lysed by sonication and the supernatant was used for caspase assay. Cleavage of the Ac-DEVD-AFC substrate was monitored every 15 min for 1 h. Viral treatment was judged to significantly contribute to variation using two-way ANOVA ($p = 0.0055$). The data were plotted using simple linear regression. Error bars indicate SEM.

3.5. MRE/rprORF Is Less Able to Infect Mosquitoes, but Replicates Normally if Infection Is Established

We then allowed mosquitoes to feed on blood containing MRE/rprORF, MRE/rpr, or MRE/control for the purpose of comparing infection prevalence and viral titer. To do this, each mosquito midgut and carcass (defined as all remaining tissues of the mosquito other than the midgut) was titered by $TCID_{50}$. In the midgut, we found that at all time points tested, the mosquitoes fed with MRE/rprORF were less likely to have detectable infection compared to MRE/rpr and MRE/control (Figure 6). Prevalence increased over time in the MRE/rprORF-fed mosquitoes, from 25% of midguts with infection at 3 days PBM to 49% at 7 days PBM. By contrast, the percentage of midgut infection in the MRE/rpr-fed mosquitoes was not found to be significantly different compared to mosquitoes that fed on MRE/control, although it was lower at 3 days PBM (65% vs. 81%). The prevalence of MRE/rpr infection also increased over time from 65% at 3 days PBM to 87% at 7 days PBM.

Midgut infection percentage in the MRE/control-fed mosquitoes reached 81% by 3 days PBM and remained high over time.

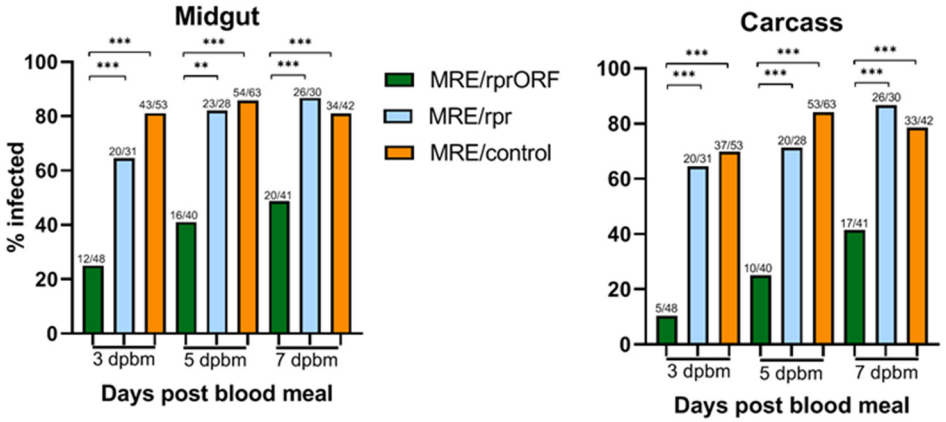

Figure 6. MRE/rprORF is less able to establish mosquito infection than MRE/rpr and MRE/control. Mosquitoes were fed blood containing MRE/rprORF, MRE/rpr, or MRE/control and dissected at 3, 5, or 7 days PBM. Midguts (**left**) and carcasses (**right**) were titered by $TCID_{50}$. Mosquitoes that did not have detectable titer were considered to be negative while any positive titer by $TCID_{50}$ was considered to be positive. Numbers above each column indicate the positive/total sample numbers. Treatments were compared using Fisher's exact test (** $p < 0.01$, *** $p < 0.001$). Statistical comparisons (brackets) are shown for all statistically significant differences.

Similar trends were seen in the percentage of mosquitoes with detectable carcass infections, representing dissemination of the virus from the midgut (Figure 6). The prevalence of mosquitoes with carcass infection in the MRE/rprORF-fed group was significantly lower compared to MRE/rpr and MRE/control at all time points tested. The percentage also increased over time and ranged from 10% at 3 days PBM to 41% at 7 days PBM. The prevalence of carcass infection in MRE/rpr-fed mosquitoes was not significantly different from MRE/control and ranged from about 65% at 3 days PBM to 87% at 7 days PBM. The percentage of carcass infection in MRE/control-fed mosquitoes was 74% at 3 days PBM with an increase to 84% at 5 days PBM and then a slight decrease to 79% at 7 days PBM. MRE/rprORF-infected mosquitoes also had lower dissemination rates than MRE/rpr and MRE/control at all time points tested (Table 1).

Table 1. Dissemination rates at different days PBM.

Virus	3 Days PBM	5 Days PBM	7 Days PBM
MRE/rprORF	41.7 [1]	62.5	85.0
MRE/rpr	100.0	87.0	100.0
MRE/control	86.1	98.2	97.1

[1] Percentage of infected mosquitoes having disseminated infection, as calculated by the number of positive carcass infections divided by the number of positive midgut infections.

To compare virus replication in the midguts and carcasses between the three groups, we focused on only those mosquitoes that had detectable titers (Figure 7). MRE/rprORF titers did not significantly differ from MRE/control at any of the time points tested in the midgut or carcass, while MRE/rpr titers were found to be higher than MRE/rprORF and MRE/control at 3 and 7 days PBM in the midgut and at 3 days PBM in the carcass. While statistical analysis of some of the titer data may have been affected by small numbers of infected mosquitoes, especially in the case of MRE/rprORF at the earlier time points, overall, there did not appear to be any large differences in titer between the three viruses.

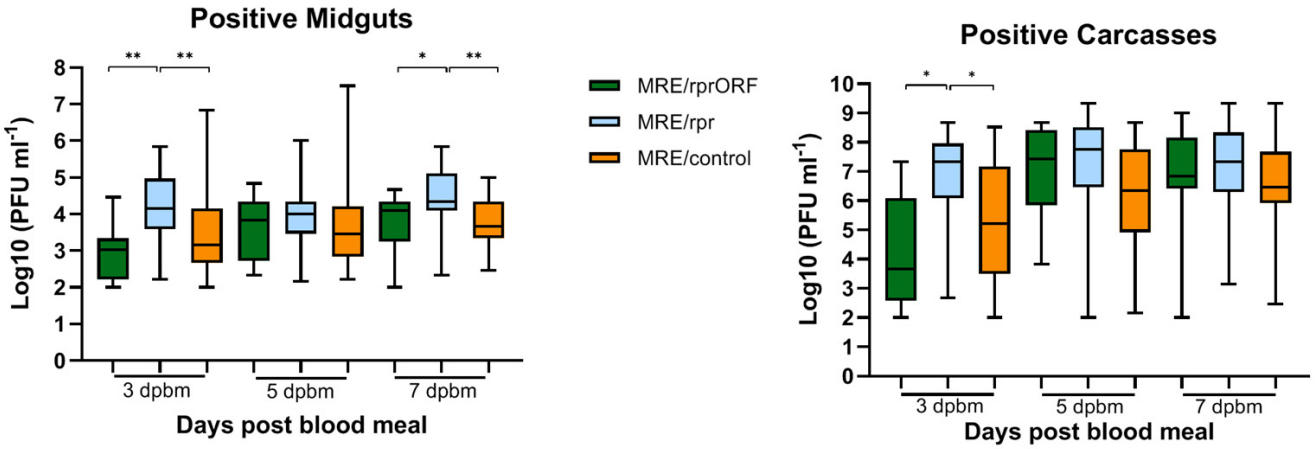

Figure 7. Mosquitoes infected with MRE/rprORF have similar titers compared to MRE/control. The titers of the infected midgut (**left**) and carcass (**right**) samples from Figure 6 are shown. Titer values were log transformed and compared by one-way ANOVA and Tukey's multiple comparisons test. * $p < 0.05$, ** $p < 0.01$. Statistical comparisons (brackets) are shown for all statistically significant differences.

3.6. Deep Sequencing Results Indicate the Reaper Insert Is Highly Stable in MRE/rprORF

To examine the stability of the *reaper* insert during mosquito infection, we performed deep sequencing of amplicons derived from the *reaper*-containing region of viral genomes present in the carcasses of 10 of the MRE/rprORF-infected mosquitoes harvested at 5 or 7 days PBM. Two independent amplicon samples were also prepared using the same stock of MRE/rprORF virus that was fed to the mosquitoes. PCR amplicons, extending from 54 nt upstream to 140 nt downstream of the Reaper ORF, were subjected to Illumina sequencing. Sequence analysis indicated that the *reaper* insert was highly stable during replication in mosquitoes, with no evidence of any deletions present at >1% frequency and only a total of five point mutations when compared to the infectious clone plasmid sequence (all pyrimidine transition mutations) being observed at greater than 1% frequency in any of the samples (Table 2). Sequencing coverage was excellent, with the minimum average read depth for any sample being 79K (Data Set S1). Two of these point mutations (C8807T and C8943T) were present in the stock virus and in all 10 mosquito samples at similarly low frequencies, and so were viewed as being irrelevant. Of the three other point mutations that were observed at >1% frequency, two (T8826C and C8844T) may be due to founder effects that occurred during midgut infection or midgut escape, since they were each observed to increase in frequency in only a single mosquito, and they were also present in the stock samples at <1% frequency. More interesting was mutation C8937T, which was present at >1% in three of the mosquitoes. In mosquito C36, C8937T was present at only 1.4%. However, in mosquitoes C17 and C37, the C8937T mutation was overwhelmingly dominant (99.5%). Change of C8937 to T results in a predicted change in amino acid 40 of Reaper, which is in the GH3 domain, a domain that has been implicated as playing a relatively minor role in induction of apoptosis [38]. However, position L40 is not well conserved within the GH3 domains of Reaper-like proteins [38,39], making the significance of this mutation unclear. Nonetheless, overall, the *reaper* insert was remarkably stable during replication in mosquitoes, especially when compared to the MRE/rpr virus [19].

Table 2. Mutations detected at >1% frequency in MRE/rprORF stock virus and infected mosquito carcasses.

Mutation	Aa Change [1]	S1 [2]	S2	C6	C9	C11	C17	C18	C19	C20	C24	C36	C37
C8807T	none	0.0265 [3]	0.0249	0.0242	0.0243	0.0265	0.0268	0.0256	0.0257	0.0248	0.0222	0.0219	0.0259
T8826C	L73P (ubi)							0.2832					
C8844T	A4V (rpr)								0.7778				
C8937T	L40P (rpr)						0.9950					0.0143	0.9946
C8943T	T37I (rpr)	0.0135	0.0143	0.0132	0.0140	0.0143	0.0139	0.0138	0.0142	0.0142	0.0142	0.0147	0.0138

[1] Predicted amino acid changes caused by point mutations in ubiquitin (ubi) or Reaper (rpr). Numbers represent the affected amino acid position in the protein and letters represent the predicted change. For example, L73P was a change from leucine to proline at position 73 of ubiquitin. [2] Samples S1 and S2 were independent RNA extractions from MRE/rprORF stock virus, while samples C6–C37 were MRE/rprORF-infected carcasses. [3] Frequency of mutation observed in sample. The minimum average read depth in any of the samples was 79 K. Blank spaces indicate that the mutation was present at <1%.

4. Discussion

In order to better understand the effects of apoptosis on the ability of SINV to infect *Ae. aegypti*, we generated a SINV construct that expresses Reaper as an in-frame insertion in the structural ORF and tested how this virus behaved in cell culture and in mosquitoes. Previous work using a SINV construct that expressed Reaper from a duplicated subgenomic promoter (MRE/rpr) found that less mosquitoes developed disseminated infection than a control virus at early time points, but this difference disappeared over time due to deletions that accumulated in the inserted *reaper* sequence [19]. Therefore, we were interested in learning what affect apoptosis would have on SINV infection if the Reaper protein was expressed in a potentially more stable fashion.

The results of our study showed that expressing the Reaper protein from the structural ORF of SINV using a ubiquitin fusion strategy was successful. We were able to detect Reaper protein in MRE/rprORF-infected cells by immunoblotting, as well as increased markers of apoptosis in both infected cells and mosquito midgut. We detected what was likely the free Reaper protein at 48 hpi but also detected what was most likely the uncleaved ubiquitin-Reaper fusion protein at both 24 hpi and 48 hpi. Thus, it appears that cleavage of ubiquitin fusion proteins in this system is relatively inefficient, although our ability to detect the cleaved, free Reaper protein may have been negatively impacted by its ability to induce cell death. We also observed a larger band of unknown origin in the MRE/control virus, which suggests that the ubiquitin expressed from these constructs may be utilized as a substrate by cellular ubiquitin ligases. We cannot conclude with certainty whether the expression of ubiquitin from the virus has any effect on virus structure or replication. However, the results of the replication curve experiments indicated that the ubiquitin fusion strategy did not result in any significant replication defects. In BHK-21 cells, MRE/control replicated to the highest level, with MRE/rprORF and MRE/rpr replicating to modestly lower levels before decreasing after 3 dpi. Although SINV infection alone causes apoptosis in BHK-21 cells [40,41], Reaper expression also induces apoptosis in mammalian cells, at least partially due to global suppression of protein synthesis [42], which might explain why the Reaper-expressing viruses replicated to lower titers than MRE/control in these cells.

In the cumulative replication curve in C6/36 cells, the differences between MRE/control and the Reaper-expressing viruses were more pronounced. This was expected since SINV does not itself cause very much death in these cells, instead establishing a persistent infection [23]. In this experiment, the titers of MRE/rprORF and MRE/rpr closely matched each other, suggesting that neither the location of the *reaper* insert nor the expression of ubiquitin affected replication. In the C6/36 noncumulative replication curve, the titers of MRE/control, MRE/rprORF, and MRE/rpr closely aligned until 3 dpi, after which it appears that enough Reaper protein had accumulated to cause significant cell death and a decrease in titer was seen. MRE/rprORF titers decreased after 3 dpi to a greater extent than those of MRE/rpr, and these two replication curves were found to be significantly different. The reason for this is unknown but it is consistent with the higher level of caspase

activity in MRE/rprORF-infected midgut compared to MRE/rpr. Thus, instability of the *reaper* insert in MRE/rpr may have decreased its effectiveness in causing cell death both in cultured cells and in mosquito midgut. It is important to note that C6/36 cells have an impaired RNAi response and therefore results in these cells may not completely reflect the in vivo situation [43].

In mosquitoes, MRE/rprORF had a decreased ability to establish both midgut and carcass infection compared to MRE/rpr. At all time points tested, MRE/rprORF caused a lower infection prevalence compared to both MRE/control and MRE/rpr, while the prevalence of MRE/rpr infection did not significantly differ from MRE/control at any of the time points. This latter result differed from our previous study, which found that the percentage of mosquitoes infected with MRE/rpr was lower than the control virus used in that study at early time points in both the midgut and the carcass [19]. Although we observed that MRE/rpr infection prevalence was lower than MRE/control at 3 dpi (65% vs. 81%), this difference did not reach statistical significance. Perhaps additional replicates would accentuate this difference. It is also possible that this difference could be due to the fact that different control viruses were used in the two studies. Regardless, the most important result for the purposes of this study was that MRE/rprORF showed significantly less ability to establish infection in the midgut and disseminate compared to MRE/rpr. We conclude that this is likely due to selective pressure to retain the *reaper* insert in the structural ORF, since deletions within the *reaper* insert would theoretically have a 2 out of 3 chance of altering the reading frame and eliminating expression of the downstream envelope proteins, resulting in defective virus. In contrast, any deletions within the *reaper* insert of MRE/rpr virus would not be expected to impact virus viability. Indeed, our deep sequencing data demonstrated that the *reaper* insert was more stably retained in MRE/rprORF than in MRE/rpr [19], and all of our results are consistent with this being the case.

The results of our study also differed from previous published results [19] when we examined the virus titers in mosquitoes that did become infected. We found that when MRE/rprORF was able to establish infection in the midgut, the titers were similar to MRE/control and this pattern continued in the carcass. It is possible that if the virus is able to accumulate to a certain level in midgut cells of some mosquitoes, apoptosis may no longer be able to effectively limit viral replication and spread. Another unexpected result was the observation that the titers of mosquitoes that became infected with MRE/rpr were higher compared to MRE/rprORF and MRE/control in the midguts at 3 and 7 days PBM and at 3 days PBM in the carcass. Deep sequencing data from our 2015 study indicated that most MRE/rpr-infected mosquitoes contain a high frequency of viruses with deletions in *reaper* [19], so this would be expected to allow it to replicate to higher levels compared to MRE/rprORF, but it is unclear why the titers were higher than MRE/control. In any case, none of the three viruses appeared to have a large replication advantage over the others in infected mosquitoes.

Deep sequencing of MRE/rprORF-infected mosquitoes demonstrated that *reaper* was much more stably maintained during infection compared to MRE/rpr [19], with no evidence of any deletions accumulating at >1% frequency in MRE/rprORF. However, in two mosquitoes, a point mutation in Reaper, T8937C, became dominant in the population. This point mutation changes an amino acid (L40) in the GH3 domain of Reaper. There is published evidence indicating that the Reaper GH3 domain plays a supportive role in inducing apoptosis, although it appears to be less important than the IBM [38]. While position L40 is located within the GH3 domain, it is not well conserved in the GH3 domains of Reaper-like proteins from Drosophilids, mosquitoes, or lepidoptera [38,39], so the effect of this mutation on Reaper-induced apoptosis is unclear. Nonetheless, the observation that this mutation became highly dominant in two mosquitoes makes it tempting to speculate that the T8937C mutation may confer a selective advantage compared to MRE/rprORF. However, the T8937C mutation was also detected in all other sequenced samples (at 1.4% in one mosquito and at <1% in the MRE/rprORF stock and the other seven mosquitoes;

Data Set S1), so if it provides a selective advantage, it is unclear why it did not predominate in more than two of the ten mosquitoes. Overall, despite this single point mutation becoming dominant in two mosquitoes, the sequencing results indicate remarkably little change in the *reaper* insert of MRE/rprORF during infection, especially when compared to the extensive loss of *reaper* that was observed in MRE/rpr.

Our results demonstrate that expression of the pro-apoptotic Reaper protein negatively affects midgut infection and dissemination by SINV. While we cannot completely rule out other explanations for this effect, it is most likely due to induction of apoptosis by Reaper. This conclusion is supported by our previous work with MRE/rpr (showing increased midgut TUNEL staining) as well as several other studies [18–21]. However, there have been studies which suggest a seemingly opposite conclusion. In one study where expression of AeIAP1, which inhibits apoptosis, was knocked down in mosquitoes, both midgut infection and dissemination increased [22]. However, AeIAP1 knockdown caused a high mortality rate and extensive pathology of the midgut tissue was observed. The systemic induction of apoptosis thus likely greatly decreased the structural integrity of the midgut, which may have allowed viral passage through the tissue. In the present study as well as in O'Neill et al. [19], the pro-apoptotic gene was inserted into the viral genome, ensuring that apoptosis was stimulated only in infected cells. Additionally, two studies have shown that knockdown of the caspase AeDronc has the opposite effect than would be expected if apoptosis was strictly antiviral, as it reduces infection with SINV or DENV-2 [22,44]. While Eng et al [44] provided evidence that AeDronc may play a role in autophagy, a process that may be important for arbovirus infection, another possible explanation for this result is that caspases are involved in remodeling of midgut basal lamina [45], which appears to be necessary for viral midgut escape [46]. Thus, either a low basal level of midgut caspase activity or extensive, widespread stimulation of apoptosis may be advantageous for a virus, while stimulation of apoptosis specifically in infected cells has a negative effect.

There are several limitations of our study which could be explored and improved upon in future studies. In this study, we only looked at the effect of Reaper expression on SINV in *Ae. aegypti*. This should be explored in other virus/vector combinations to determine if the results of this study are generalizable to other situations. Additionally, while less than 50% of mosquitoes exposed to MRE/rprORF developed disseminated infection by 7 days PBM, we did see this percentage increase from 3 to 7 days PBM. It is possible that at further time points the percentage of infection of MRE/rprORF would become equivalent to the control. The durability of this effect should be further explored in the future.

Overall, this study provides additional evidence that expression of the pro-apoptotic protein Reaper has a negative effect on the ability of SINV to establish infection in the midgut and disseminate to the carcass. Expressing Reaper by inserting the gene into the structural ORF caused a more robust and durable reduction in infection prevalence than expression via the duplicated subgenomic promoter, with the differences in both midgut and carcass infection prevalence between MRE/rprORF and MRE/control being significant at all of the time points tested. These results provide additional evidence that the apoptotic pathway is antiviral in mosquitoes and possibly could be exploited to prevent transmission of arboviruses. Additionally, this study is consistent with previous findings that inserting genes into a viral ORF is a useful strategy for expression of genes that are subject to negative selection.

Supplementary Materials: The following supporting information can be downloaded at: https://www.mdpi.com/article/10.3390/v14092035/s1, Figure S1: Image of full immunoblot in Figure 2; Data Set S1, sequencing results indicating read variants at each nucleotide position in the twelve amplicon samples.

Author Contributions: Conceptualization, A.C. and R.J.C.; validation, A.C.; formal analysis, A.C., S.R.S. and R.J.C.; investigation, A.C.; writing—original draft preparation, A.C.; writing—review and editing, A.C., S.R.S. and R.J.C.; visualization, A.C.; supervision, R.J.C.; project administration, R.J.C.; funding acquisition, R.J.C. All authors have read and agreed to the published version of the manuscript.

Funding: This research received no external funding.

Institutional Review Board Statement: Not applicable.

Informed Consent Statement: Not applicable.

Data Availability Statement: Illumina sequence data have been deposited in the Sequence Read Archive under BioProject ID PRJNA875102. The remaining data are available from the corresponding author upon reasonable request.

Acknowledgments: The authors thank Emma Francis, Abbey Phelps, Misty Bear, and Jessica Rakijas for technical assistance, Peter Hodoameda for preparing the PCR amplicons for sequencing, and Alina Akhunova (K-State Integrated Genomics Facility) for assistance with Illumina sequencing. A.C. received partial stipend support from the Johnson Cancer Research Center at Kansas State University. This research was also supported by the Mary L. Vanier Endowed Professorship Fund and by the Kansas Agricultural Experiment Station. This is contribution 22-184-J from the Kansas Agricultural Experiment Station.

Conflicts of Interest: The authors declare no conflict of interest. The funders had no role in the design of the study; in the collection, analyses, or interpretation of data; in the writing of the manuscript; or in the decision to publish the results.

References

1. Pan American Health Organization/World Health Organization. *Epidemiological Update: Yellow Fever, Situation Summary in the Americas*; Pan Health Organization/World Health Organization: Washington, DC, USA, 2018. Available online: https://www3.paho.org/hq/index.php?option=com_docman&view=download&category_slug=yellow-fever-2194&alias=44111-20-march-2018-yellow-fever-epidemiological-update-111&Itemid=270&lang=en (accessed on 7 December 2021).
2. Morrison, T.E. Reemergence of chikungunya virus. *J. Virol.* **2014**, *88*, 11644–11647. [CrossRef] [PubMed]
3. Murray, C.J.L.; Barber, R.M.; Foreman, K.J.; Abbasoglu Ozgoren, A.; Abd-Allah, F.; Abera, S.F.; Aboyans, V.; Abraham, J.P.; Abubakar, I.; Abu-Raddad, L.J.; et al. Global, regional, and national disability-adjusted life years (DALYs) for 306 diseases and injuries and healthy life expectancy (HALE) for 188 countries, 1990–2013: Quantifying the epidemiological transition. *Lancet* **2015**, *386*, 2145–2191. [CrossRef]
4. Colón-González, F.J.; Sewe, M.O.; Tompkins, A.M.; Sjödin, H.; Casallas, A.; Rocklöv, J.; Caminade, C.; Lowe, R. Projecting the risk of mosquito-borne diseases in a warmer and more populated world: A multi-model, multi-scenario intercomparison modelling study. *Lancet Planet Health* **2021**, *5*, e404–e414. [CrossRef]
5. Bouchard, C.; Dibernardo, A.; Koffi, J.; Wood, H.; Leighton, P.; Lindsay, L. Climate change and infectious diseases: The challenges: N increased risk of tick-borne diseases with climate and environmental changes. *Can. Commun. Dis. Rep.* **2019**, *45*, 83. [CrossRef]
6. Liu-Helmersson, J.; Quam, M.; Wilder-Smith, A.; Stenlund, H.; Ebi, K.; Massad, E.; Rocklöv, J. Climate change and *Aedes* vectors: 21st century projections for dengue transmission in Europe. *EBioMedicine* **2016**, *7*, 267–277. [CrossRef]
7. Deming, R.; Manrique-Saide, P.; Medina Barreiro, A.; Cardenã, E.U.K.; Che-Mendoza, A.; Jones, B.; Liebman, K.; Vizcaino, L.; Vazquez-Prokopec, G.; Lenhart, A. Spatial variation of insecticide resistance in the dengue vector *Aedes aegypti* presents unique vector control challenges. *Parasit. Vectors* **2016**, *9*, 67. [CrossRef]
8. Weill, M.; Luffalla, G.; Mogensen, K.; Chandre, F.; Berthomieu, A.; Berticat, C.; Pasteur, N.; Philips, A.; Fort, P.; Raymond, M. Insecticide resistance in mosquito vectors. *Nature* **2003**, *423*, 136–137. [CrossRef]
9. Moyes, C.L.; Vontas, J.; Martins, A.J.; Ng, L.C.; Koou, S.Y.; Dusfour, I.; Raghavendra, K.; Pinto, J.; Corbel, V.; David, J.-P.; et al. Contemporary status of insecticide resistance in the major *Aedes* vectors of arboviruses infecting humans. *PLoS Negl. Trop. Dis.* **2017**, *11*, e0005625. [CrossRef]
10. Franz, A.W.; Kantor, A.; Passarelli, A.L.; Clem, R.J. Tissue barriers to arbovirus infection in mosquitoes. *Viruses* **2015**, *7*, 3741–3767. [CrossRef] [PubMed]
11. Blair, C.D.; Olson, K.E. Mosquito immune responses to arbovirus infections. *Curr. Opin. Insect Sci.* **2014**, *3*, 22–29. [CrossRef]
12. Clarke, T.E.; Clem, R.J. Insect defenses against virus infection: The role of apoptosis. *Int. Rev. Immunol.* **2003**, *22*, 401–424. [CrossRef] [PubMed]
13. Liu, Q.; Clem, R.J. Defining the core apoptosis pathway in the mosquito disease vector *Aedes aegypti*: The roles of iap1, ark, dronc, and effector caspases. *Apoptosis* **2011**, *16*, 105–113. [CrossRef] [PubMed]

14. Wang, H.; Clem, R.J. The role of IAP antagonist proteins in the core apoptosis pathway of the mosquito disease vector *Aedes aegypti*. *Apoptosis* **2011**, *16*, 235–248. [CrossRef] [PubMed]
15. Hoffmann, J.A. The immune response of Drosophila. *Nature* **2003**, *426*, 33–38. [CrossRef] [PubMed]
16. Bryant, B.; Blair, C.D.; Olson, K.E.; Clem, R.J. Annotation and expression profiling of apoptosis-related genes in the yellow fever mosquito, *Aedes aegypti*. *Insect Biochem. Mol. Biol.* **2008**, *38*, 331–345. [CrossRef]
17. Chai, J.; Yan, N.; Huh, J.R.; Wu, J.-W.; Li, W.; Hay, B.A.; Shi, Y. Molecular mechanism of Reaper-Grim-Hid-mediated suppression of DIAP1-dependent Dronc ubiquitination. *Nat. Struct. Mol. Biol.* **2003**, *10*, 892–898. [CrossRef] [PubMed]
18. Vaidyanathan, R.; Scott, T.W. Apoptosis in mosquito midgut epithelia associated with West Nile virus infection. *Apoptosis* **2006**, *11*, 1643–1651. [CrossRef]
19. O'Neill, K.; Huang, N.; Unis, D.; Clem, R.J. Rapid selection against arbovirus-induced apoptosis during infection of a mosquito vector. *Proc. Natl. Acad. Sci. USA* **2015**, *112*, E1152–E1161. [CrossRef]
20. Ocampo, C.B.; Caicedo, P.A.; Jaramillo, G.; Ursic Bedoya, R.; Baron, O.; Serrato, I.M.; Cooper, D.M.; Lowenberger, C. Differential expression of apoptosis related genes in selected strains of *Aedes aegypti* with different susceptibilities to dengue virus. *PLoS ONE* **2013**, *8*, e61187. [CrossRef]
21. Ayers, J.B.; Coatsworth, H.G.; Kang, S.; Dinglasan, R.R.; Zhou, L. Clustered rapid induction of apoptosis limits ZIKV and DENV-2 proliferation in the midguts of *Aedes aegypti*. *Commun. Biol.* **2021**, *4*, 69. [CrossRef]
22. Wang, H.; Gort, T.; Boyle, D.L.; Clem, R.J. Effects of manipulating apoptosis on Sindbis virus infection of *Aedes aegypti* mosquitoes. *J. Virol.* **2012**, *86*, 6546–6554. [CrossRef] [PubMed]
23. Wang, H.; Blair, C.D.; Olson, K.E.; Clem, R.J. Effects of inducing or inhibiting apoptosis on Sindbis virus replication in mosquito cells. *J. Gen. Virol.* **2008**, *89*, 2651–2661. [CrossRef] [PubMed]
24. Thomas, J.M.; Klimstra, W.B.; Ryman, K.D.; Heidner, H.W. Sindbis virus vectors designed to express a foreign protein as a cleavable component of the viral structural polyprotein. *J. Virol.* **2003**, *77*, 5598–5606. [CrossRef]
25. Carpenter, A.; Bryant, W.B.; Santos, S.R.; Clem, R.J. Infection of *Aedes aegypti* mosquitoes with midgut-attenuated Sindbis virus reduces, but does not eliminate, disseminated infection. *J. Virol.* **2021**, *95*, 136–157. [CrossRef] [PubMed]
26. Donnelly, M.L.L.; Luke, G.; Mehrotra, A.; Li, X.; Hughes, L.E.; Gani, D.; Ryan, M.D. Analysis of the aphthovirus 2A/2B polyprotein "cleavage" mechanism indicates not a proteolytic reaction, but a novel translational effect: A putative ribosomal "skip". *J. Gen. Virol.* **2001**, *82*, 1013–1025. [CrossRef]
27. Hunter, A.M.; Kottachchi, D.; Lewis, J.; Duckett, C.S.; Korneluk, R.G.; Liston, P. A novel ubiquitin fusion system bypasses the mitochondria and generates biologically active Smac/DIABLO. *J. Biol. Chem.* **2003**, *278*, 7494–7499. [CrossRef]
28. Baker, R.T. Protein expression using ubiquitin fusion and cleavage. *Curr. Opin. Biotechnol.* **1996**, *7*, 541–546. [CrossRef]
29. O' Reilly, D.R.; Miller, L.K.; Luckow, V.A. *Baculovirus Expression Vectors: A Laboratory Manual*; Oxford University Press: New York, NY, USA, 1994; 134p.
30. Heng, L. Aligning sequence reads, clone sequences and assembly contigs with BWA-MEM. *arXiv* **2013**, arXiv:1303.3997.
31. Li, H.; Handsaker, B.; Wysoker, A.; Fellell, T.; Ruan, J.; Homer, N.; Marth, G.; Abecasis, G.; Durbin, R. 1000 Genome Project Data Processing Subgroup. The sequence alignment/map format and SAMtools. *Bioinformatics* **2009**, *25*, 2078–2079. [CrossRef]
32. Khanna, A.; Larson, D.; Srivatsan, S.; Mosior, M.; Abbott, T.; Kiwala, S.; Ley, T.; Duncavage, E.; Walter, M.; Walker, J.; et al. Bam-readcount—Rapid generation of basepair-resolution sequence metrics. *J. Open Source Softw.* **2022**, *69*, 3722. [CrossRef]
33. Foy, B.D.; Myles, K.M.; Pierro, D.J.; Sanchez-Vargas, I.; Uhlirová, M.; Jindra, M.; Beaty, B.J.; Olson, K.E. Development of a new Sindbis virus transducing system and its characterization in three Culicine mosquitoes and two Lepidopteran species. *Insect Mol. Biol.* **2004**, *13*, 89–100. [CrossRef] [PubMed]
34. Yan, N.; Wu, J.W.; Chai, J.; Li, W.; Shi, Y. Molecular mechanisms of DrICE inhibition by DIAP1 and removal of inhibition by Reaper, Hid and Grim. *Nat. Struct. Mol. Biol.* **2004**, *11*, 420–428. [CrossRef] [PubMed]
35. Wyllie, A.H.; Kerr, J.F.R.; Currie, A.R. Cell Death: The significance of apoptosis. *Int. Rev. Cytol.* **1980**, *68*, 251–306. [CrossRef] [PubMed]
36. Skalka, M.; Matyasova, J.; Cejkova, M. DNA in chromatin of irradiated lymphoid tissues degrades in vivo into regular fragments. *FEBS Lett.* **1976**, *72*, 271–274. [CrossRef]
37. Williams, J.R.; Little, J.B.; Shipley, W.U. Association of mammalian cell death with a specific endonucleolytic degradation of DNA. *Nature* **1974**, *252*, 754–755. [CrossRef]
38. Zhou, L. The 'unique key' feature of the Iap-binding motifs in RHG proteins. *Cell Death Differ.* **2005**, *12*, 1148–1151. [CrossRef]
39. Bryant, B.; Zhang, Y.; Zhang, C.; Santos, C.P.; Clem, R.J.; Zhou, L. A lepidopteran orthologue of reaper reveals functional conservation and evolution of IAP antagonists. *Insect Mol. Biol.* **2009**, *18*, 341–351. [CrossRef]
40. Levine, B.; Huang, Q.; Isaacs, J.T.; Reed, J.C.; Griffin, D.E.; Hardwick, J.M. Conversion of lytic to persistent alphavirus infection by the bcl-2 cellular oncogene. *Nature* **1993**, *361*, 739–742. [CrossRef]
41. Nava, V.E.; Rosen, A.; Veliuona, M.A.; Clem, R.J.; Levine, B.; Hardwick, J.M. Sindbis virus induces apoptosis through a caspase-dependent, CrmA-sensitive pathway. *J. Virol.* **1998**, *72*, 452–459. [CrossRef]
42. Tait, S.W.G.; Werner, A.B.; de Vries, E.; Borst, J. Mechanism of action of Drosophila Reaper in mammalian cells: Reaper globally inhibits protein synthesis and induces apoptosis independent of mitochondrial permeability. *Cell Death Differ.* **2004**, *11*, 800–811. [CrossRef]

43. Brackney, D.E.; Scott, J.C.; Sagawa, F.; Woodward, J.E.; Miller, N.A.; Schilkey, F.D.; Mudge, J.; Wilusz, J.; Olson, K.E.; Blair, C.D.; et al. C6/36 *Aedes albopictus* cells have a dysfunctional antiviral RNA interference response. *PLoS Negl. Trop. Dis.* **2010**, *4*, e856. [CrossRef] [PubMed]
44. Eng, M.W.; van Zuylen, M.N.; Severson, D.W. Apoptosis-related genes control autophagy and influence DENV-2 infection in the mosquito vector, *Aedes aegypti*. *Insect Biochem. Mol. Biol.* **2016**, *76*, 70–83. [CrossRef] [PubMed]
45. Means, J.C.; Passarelli, A.L. Viral fibroblast growth factor, matrix metalloproteases, and caspases are associated with enhancing systemic infection by baculoviruses. *Proc. Natl. Acad. Sci. USA* **2010**, *107*, 9825–9830. [CrossRef] [PubMed]
46. Dong, S.; Balaraman, V.; Kantor, A.M.; Lin, J.; Grant, D.A.G.; Held, N.L.; Franz, A.W.E. Chikungunya virus dissemination from the midgut of *Aedes aegypti* is associated with temporal basal lamina degradation during bloodmeal digestion. *PLoS Negl. Trop. Dis.* **2017**, *11*, e0005976. [CrossRef]